

Article

Plumbagin Modulates Leukemia Cell Redox Status

François Gaascht^{1,†}, Marie-Hélène Teiten^{1,†}, Claudia Cerella¹, Mario Dicato¹,
Denyse Bagrel² and Marc Diederich^{3,*}

¹ Laboratoire de Biologie Moléculaire et Cellulaire du Cancer (LBMCC), Hôpital Kirchberg, 9, Rue Edward Steichen, L-2540 Luxembourg, Grand-Duchy of Luxembourg;

E-Mails: francois.gaascht@lbmcc.lu (F.G.); marie_helene.teiten@lbmcc.lu (M.-H.T.); claudia.cerella@lbmcc.lu (C.C.); mdicato@gmail.com (M.D.)

² Laboratoire Structure et Réactivité des Systèmes Moléculaires Complexes, UMR CNRS 7565, Université de Lorraine, Campus Bridoux, Rue du Général Delestraint, F-57070 Metz, France; E-Mail: denyse.bagrel@univ-lorraine.fr

³ Department of Pharmacy, College of Pharmacy, Seoul National University, Seoul 151-742, Korea

† These authors contributed equally to this work.

* Author to whom correspondence should be addressed; E-Mail: marcdiederich@snu.ac.kr; Tel.: +82-2-880-8919.

Received: 3 June 2014; in revised form: 20 June 2014 / Accepted: 25 June 2014 /

Published: 10 July 2014

Abstract: Plumbagin is a plant naphthoquinone exerting anti-cancer properties including apoptotic cell death induction and generation of reactive oxygen species (ROS). The aim of this study was to elucidate parameters explaining the differential leukemia cell sensitivity towards this compound. Among several leukemia cell lines, U937 monocytic leukemia cells appeared more sensitive to plumbagin treatment in terms of cytotoxicity and level of apoptotic cell death compared to more resistant Raji Burkitt lymphoma cells. Moreover, U937 cells exhibited a ten-fold higher ROS production compared to Raji. Neither differential incorporation, nor efflux of plumbagin was detected. Pre-treatment with thiol-containing antioxidants prevented ROS production and subsequent induction of cell death by apoptosis whereas non-thiol-containing antioxidants remained ineffective in both cellular models. We conclude that the anticancer potential of plumbagin is driven by pro-oxidant activities related to the cellular thiolstat.

Keywords: plumbagin; natural products; leukemia; cancer; reactive oxygen species; glutathione; apoptosis; thiol groups

1. Introduction

Development of anti-cancer drug resistance and differential susceptibility of patients remain the main factors reducing the effectiveness of current chemotherapeutic treatments. Combinational therapies and the identification of novel potent and specific anti-cancer agents could contribute to improve existing therapies. However, it has become clear that a personalized approach could be the key to more effective treatments. In this view, correlative studies linking cancer patients' genetic or epigenetic [1–3] background to treatment response will be crucial for both therapeutic outcome and elucidation of unknown molecular mechanisms to eventually achieve “targeted therapies”.

Natural compounds, whether extracted from terrestrial or marine organisms, offer a large variability of molecular scaffolds with anti-cancer potential. Frequently, they derive from medicinal or dietary traditions that already provided health-promoting effects for centuries [4–7]. Amongst the best-known plant compounds, polyphenols like curcumin [8–11] or polysulfides [12–15], cardiac glycosides [16–18] were recently investigated and corresponding anticancer mechanisms were identified. Moreover interesting anti-cancer compounds from entophytic fungi were recently investigated [19,20].

Plumbagin (5-hydroxy-2-methyl-1,4-naphthoquinone) is a secondary metabolite produced by various plants (*Plumbago zeylanica*, *Dionaea muscipula*, *Nepenthes gracilis*, *Drosera binata* or *Juglans regia*) [19,21,22] and acts as a potent anti-cancer agent in various cellular cancer models, including breast, cervical, gastric, lung, melanoma, prostate cells [23–28]. A number of studies have shown that plumbagin acts on cancer cells as cell cycle inhibitor [24,28,29], cytotoxic agent [27,30–34], angiogenesis inhibitor [35,36], and as a modulator of various cancer-specific pathways (*i.e.*, mediated by NF- κ B [37,38] or mitogen activated protein kinases (MAPK) [28,29,39]). Mechanistic studies suggest that the anti-cancer effects of plumbagin depend mostly on its ubiquitous pro-oxidant activities. Accordingly, plumbagin elicits intracellular ROS in a number of cancer cell models; moreover, strategies preventing or scavenging ROS formation inhibit the biological effects ascribed [40–44]. Glutathione (GSH), the major cellular anti-oxidant, was identified as a direct target of plumbagin by its ability to bind GSH [22,45]. Indirectly, it has been suggested that plumbagin acts as an electrophile against GSH [46]. Finally, plumbagin was shown to inhibit glutathione-S-transferase (GST) [47,48]. Altogether, these findings suggest that plumbagin regulates the cellular redox state by modulation of GSH even though additional redox-dependent mechanisms could be directly or indirectly involved.

The favorable differential effect of plumbagin on cancer *vs.* healthy cell models and the confirmation of its effectiveness in *in vivo* experimental models suggest plumbagin as a promising candidate for more advanced investigations. However, further elucidation of its mechanism of action is still required especially to identify the most susceptible cancer cell models.

In this study, we analyzed the effect of plumbagin on the viability of a panel of human hematopoietic cancer cell models, including chronic and acute forms of hematological malignancies (U937, Raji, K562, Jurkat, HL-60) compared to peripheral blood mononuclear cells (PBMCs) from

healthy donors. We selected the U937 (most sensitive) and Raji (less sensitive) cells for a comparative mechanistic study. As PBMCs were not affected by the treatment, we also confirmed the excellent differential anti-cancer potential of plumbagin. Altogether, we observed that the pro-oxidant regulation is independent of a differential intake/uptake of the compound by the two cancer cell models. We rather demonstrate the differential ability of the compound to elicit ROS in U937 and Raji cells as well as to impact the intracellular GSH pool. We finally suggest a differential expression of redox-related factors as potential regulators of the observed differential susceptibility.

2. Results and Discussion

2.1. Plumbagin Reduces Leukemia Cell Viability

Evaluation of the effect of plumbagin on the viability of different leukemia cell lines by trypan blue exclusion assay revealed that this compound presents a cytotoxic effect towards all cell lines tested (Table 1). U937 cells appear as the most sensitive cell line with an IC_{50} ranging from $0.82 \pm 0.04 \mu\text{M}$ to $0.66 \pm 0.02 \mu\text{M}$ observed between 24 and 72 h of treatment. Raji cells were less sensitive with an IC_{50} value of $5.06 \pm 0.22 \mu\text{M}$ and $2.66 \pm 0.03 \mu\text{M}$ respectively after 24 and 72 h treatment. Even at the highest concentration tested ($10 \mu\text{M}$), PBMCs were not affected by plumbagin treatment. For further mechanistic studies of the effects of plumbagin, we selected U937 and Raji cells to perform a comparative analysis using IC_{50} concentrations at 24 h, respectively, $1 \mu\text{M}$ for U937 and $5 \mu\text{M}$ for Raji cells.

Table 1. Cytotoxic effect of plumbagin on different human leukemia cell lines compared to PBMCs from healthy donors. IC_{50} values were determined by three independent trypan-blue assays after 24, 48 and 72 h of treatment. The data are the mean of at least three independent experiments \pm SD. N.C. stands for “not cytotoxic” (viability > 80%) for a concentration up to $10 \mu\text{M}$.

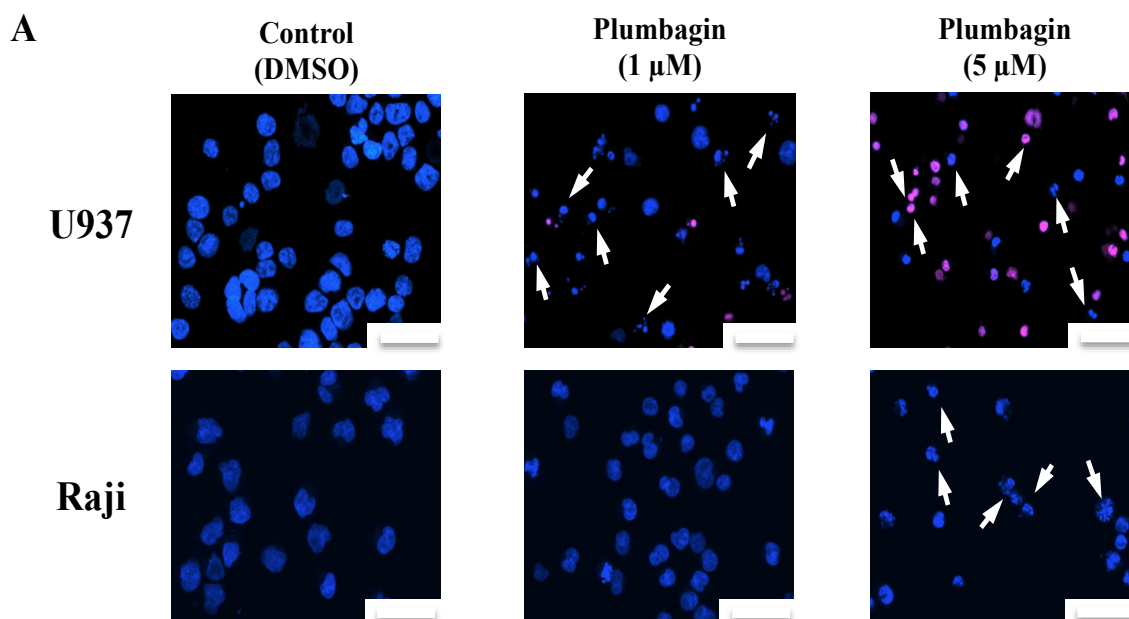
Cell Lines	IC_{50} (μM)		
	24 h	48 h	72 h
HL-60	1.38 ± 0.37	0.92 ± 0.16	0.90 ± 0.13
Jurkat	2.20 ± 1.07	0.98 ± 0.15	0.86 ± 0.16
K562	1.07 ± 0.33	0.90 ± 0.32	0.89 ± 0.30
Raji	5.06 ± 0.22	3.49 ± 0.12	2.66 ± 0.03
U937	0.82 ± 0.04	0.68 ± 0.01	0.66 ± 0.02
PBMC	N.C.	N.C.	

2.2. Plumbagin Induces Apoptotic Cell Death

Considering the elevated levels of cytotoxicity, we analyzed the type of cell death triggered by plumbagin in U937 and Raji cells by fluorescence microscopy after staining with Hoechst and propidium iodide (PI). 24 h of treatment at a concentration of $1 \mu\text{M}$ (U937) and $5 \mu\text{M}$ (Raji) induced the appearance of nuclear morphological alterations compatible with apoptosis in both cell lines (Figure 1A,B). This finding was further confirmed by the analysis of the exposure of phosphatidylserine by Annexin V/PI assay (Figure 1C,D). Results pointed out that both cell lines died by an apoptotic process in a dose-dependent manner. These results were confirmed by Western-blot analysis that

showed caspase cleavage and decrease Mcl-1 and Bcl-2 anti-apoptotic protein expression levels, starting from the respective IC_{50} concentration of plumbagin in U937 and Raji cells (Figure 2A). Pre-treatment with the pan-caspase activity inhibitor (Z-VAD-FMK) prevented the 17–10 kDa caspase-3 fragment formation. This result confirms that plumbagin induces cell death by a caspase-dependent apoptotic process (Figure 2B). These results have been confirmed by fluorescence microscopy analysis after Hoechst staining (data not shown).

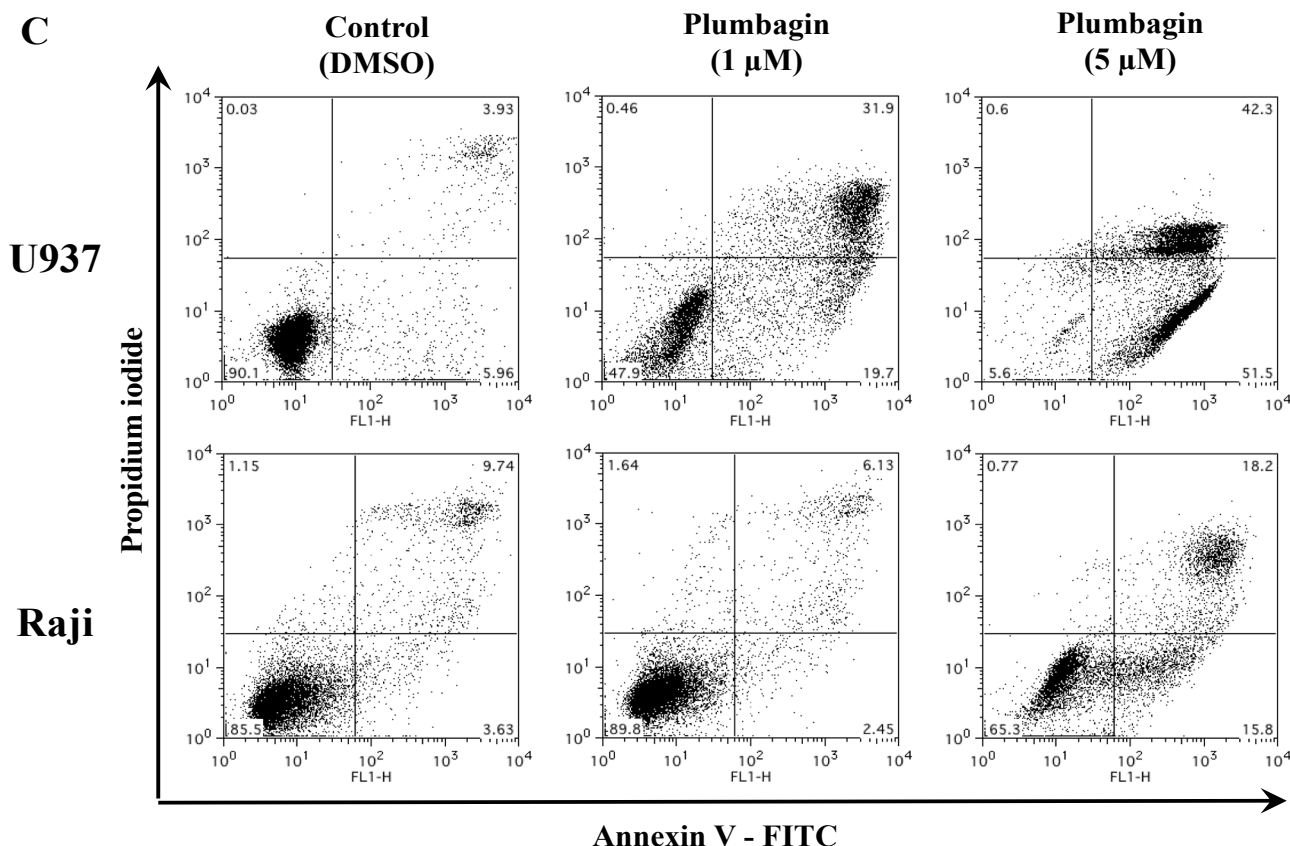
Figure 1. Cell death was assessed in U937 and Raji cells treated with plumbagin for 24 h at concentrations corresponding to their respective IC_{50} values. (A,B) Double staining with Hoechst and propidium iodide (PI) (the images shown are representative for at least three independent experiments); scale at the lower right corner = 100 μ m. Arrows point to cells showing apoptotic features after plumbagin treatment; (C,D) Annexin V/PI staining and flow cytometry analysis (one of three experiments shown). Cell population corresponding to early and late (in secondary necrosis) apoptotic cells are respectively in the lower and upper right quadrants. All results presented are the mean \pm SD of at least three independent experiments. The values in both tables correspond to percentage of apoptotic cells of at least three independent experiments. * $p < 0.05$, ** $p < 0.01$ and *** $p < 0.001$ compared to non-treated cells, respectively.



B

Cell lines	Control (DMSO)	Plumbagin (1 μ M)	Plumbagin (5 μ M)
U937	2.65 \pm 1.01	54.18 \pm 5.70 (**)	81.08 \pm 5.12 (***)
Raji	4.12 \pm 2.55	13.49 \pm 3.74 (*)	46.71 \pm 4.48 (***)

Figure 1. Cont.



D

Cell lines	Control (DMSO)	Plumbagin (1 μM)	Plumbagin (5 μM)
U937	9.89 ± 2.14	51.6 ± 4.90 (**)	93.9 ± 4.21 (**)
Raji	12.81 ± 0.49	11.95 ± 2.92	37.47 ± 13.54 (*)

2.3. Plumbagin Induces Different Levels of Intracellular ROS in U937 vs. Raji Cells

Published data demonstrated the capacity of plumbagin to elicit ROS in cancer cells [26,27,49]. Analysis of intracellular ROS production in U937 and Raji cells exposed to plumbagin was performed by flow cytometry analysis after staining with 2',7'-dichlorodihydrofluorescein diacetate (H₂DCFDA). As shown in Figure 3A,B, plumbagin induces ROS production in both cell lines tested. U937 cells show a very robust increase in intracellular ROS already after 15 min treatment at 1 μM plumbagin. Raji cells, in contrast, show a much milder intracellular ROS increase compared to the positive control hydrogen peroxide (H₂O₂, 50 μM). The level of ROS production induced by plumbagin is ten-fold higher in U937 compared to Raji cells. The incubation of Raji cells with a lower, sub-apoptogenic, concentration of plumbagin (1 μM) showed a comparable level of ROS production. The flow cytometry analysis did not reveal any cell subpopulations differently responsive to ROS production, therefore indicating a homogenous ability of cells to increase ROS production upon treatment. Moreover, no significant changes in ROS production were observed for longer incubation times with both cell lines. These results suggest that the differential plumbagin-induced ROS production is an early event.

Figure 2. Effect of plumbagin on pro- and anti-apoptotic cell markers. **(A)** Caspase activation and expression of anti-apoptotic Mcl-1 and Bcl-2 markers were analyzed by Western-Blot after 16 h of treatment by plumbagin; **(B)** Pre-treatment with Z-VAD-FMK (50 μ M), a pan-caspase activity inhibitor. Western Blot analysis (left panel); fluorescence microscope observations upon double staining with Hoechst. Arrows point to cells showing apoptotic features after plumbagin treatment (right panel). C: control, Z: Z-VAD-FMK, P: plumbagin (1 μ M), Z/P: cells pre-treated with Z-VAD-FMK and then treated with plumbagin (1 μ M). U937 cells treated with VP16 were used as apoptosis positive control. Results are representative of at least three independent experiments.

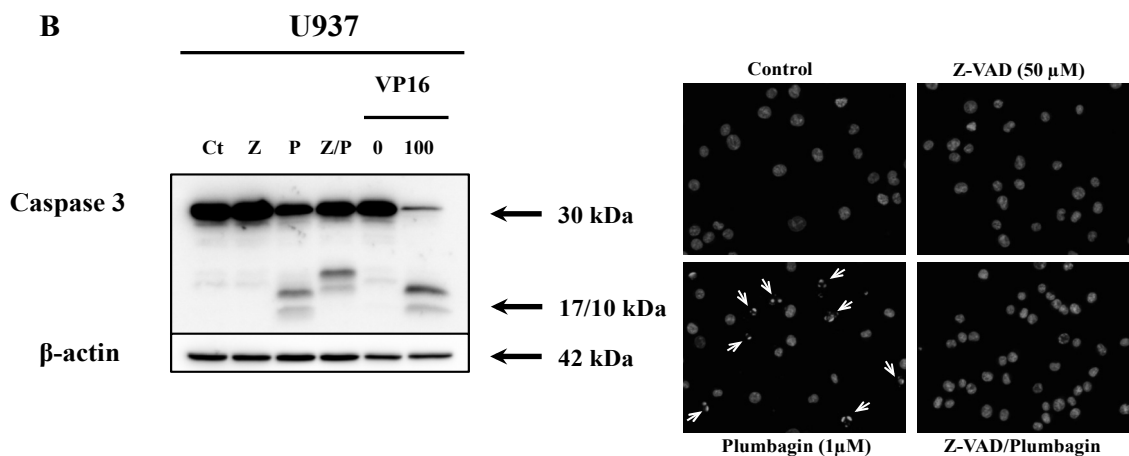
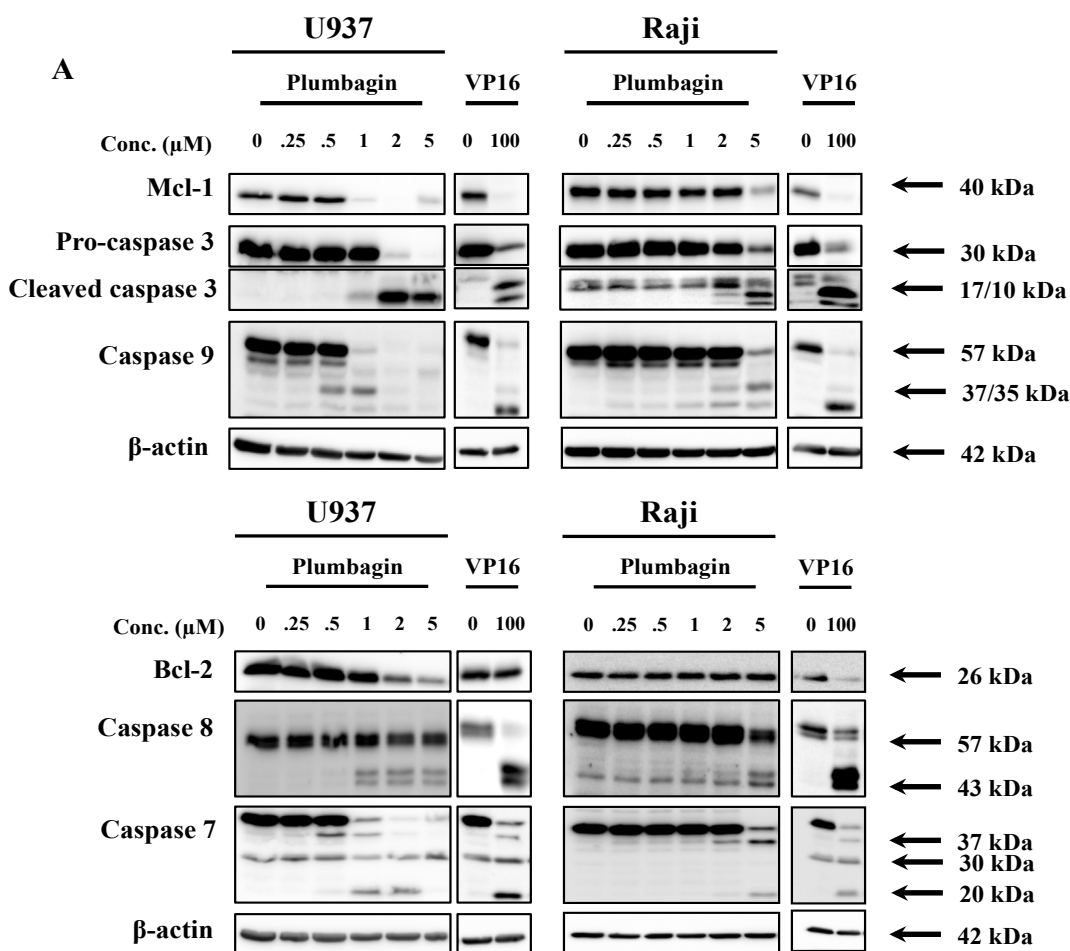
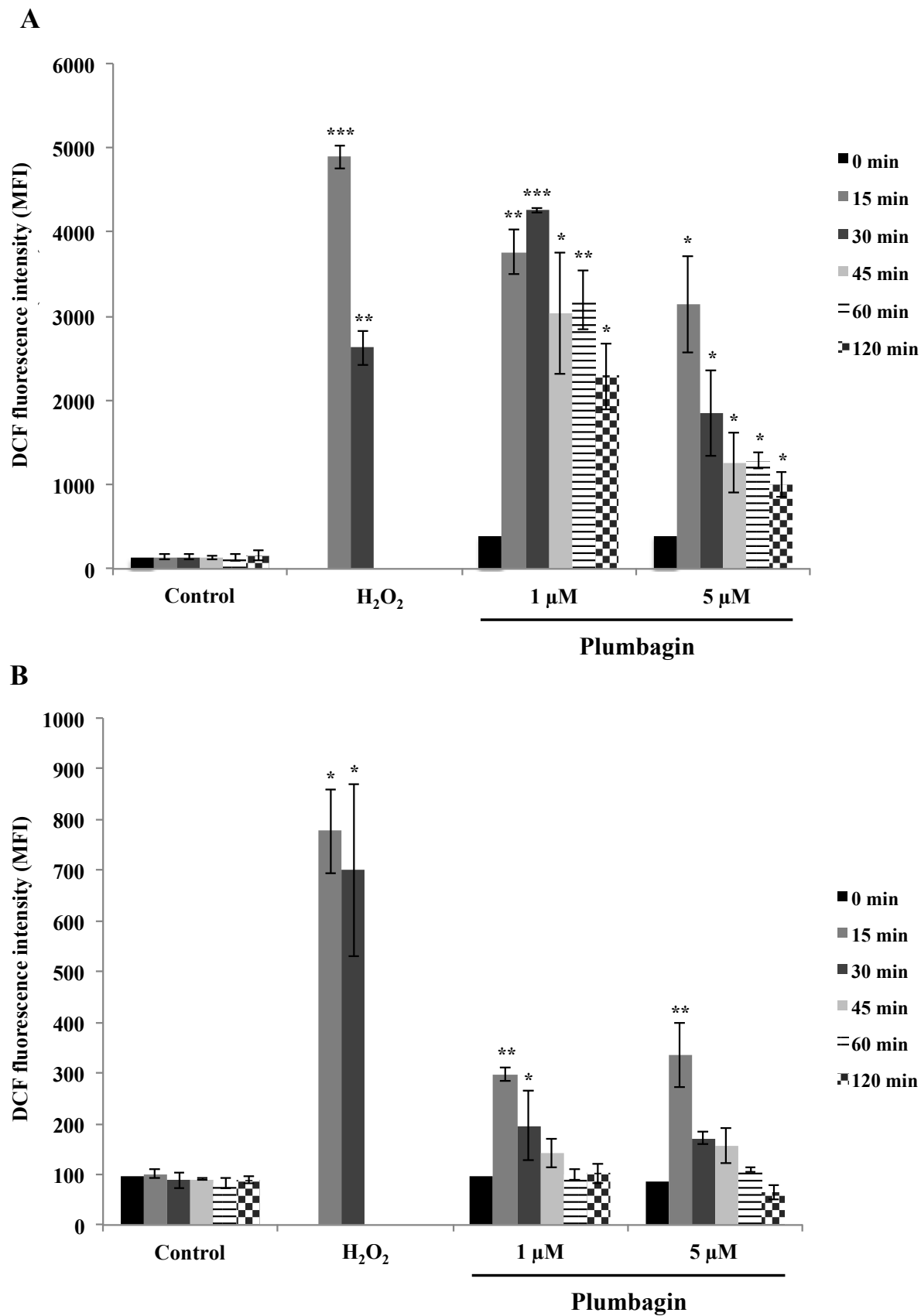


Figure 3. Time-course analysis of ROS measured in U937 (A) and Raji (B) cells upon treatment with plumbagin was assessed with 2',7'-dichlorodihydrofluorescein diacetate (H₂DCFDA). Results are the mean ± SD of at least three independent experiments. * *p* < 0.05, ** *p* < 0.01 and *** *p* < 0.001 compared to non-treated cells, respectively.



2.4. Differential ROS Generation Is not a Consequence of a Different Uptake/Efflux of Plumbagin

The observed ROS generation could be the consequence of a differential internalization of plumbagin. As plumbagin is a fluorescent pigment [45], we then investigated differential internalization. Analysis of the intracellular fluorescence of plumbagin by flow cytometry (see “Experimental” section) revealed that this compound accumulates similarly in U937 and Raji cell lines as a function of incubation time (Figure 4A). Besides, in the drug-efflux test, no decrease of the plumbagin-generated intracellular fluorescence was observed in both cell lines up to 90 min of incubation in plumbagin-free culture medium (recovery). Fluorescence maintained very high levels up to 4 h (not shown) without any difference depending on the cell models. Untreated cells did not show any modulation of fluorescence over the time as expected (data not shown). This aspect may reveal specific aspects related to the intracellular metabolism of the compound and may deserve future investigations, beyond the scope of this study. Altogether, we can exclude a differential internalization or efflux of the compound as the responsible factor for lower ROS levels in Raji.

Figure 4. (A) Plumbagin uptake assay was performed after treatment of cells at 5 μ M. Samples were collected and analyzed by flow cytometry without additional staining; (B) Plumbagin efflux assay was performed after 30 min of incubation with the same concentration of plumbagin used for the uptake assay, followed by recovery in plumbagin-free medium (see “Experimental” section) [50]. U937 and Raji cells were collected at indicated times and their auto-fluorescence was analyzed by flow cytometry. Untreated cells did not show any modulation of fluorescence over the time as expected (data not shown). Results are the mean \pm SD of at least three independent experiments.

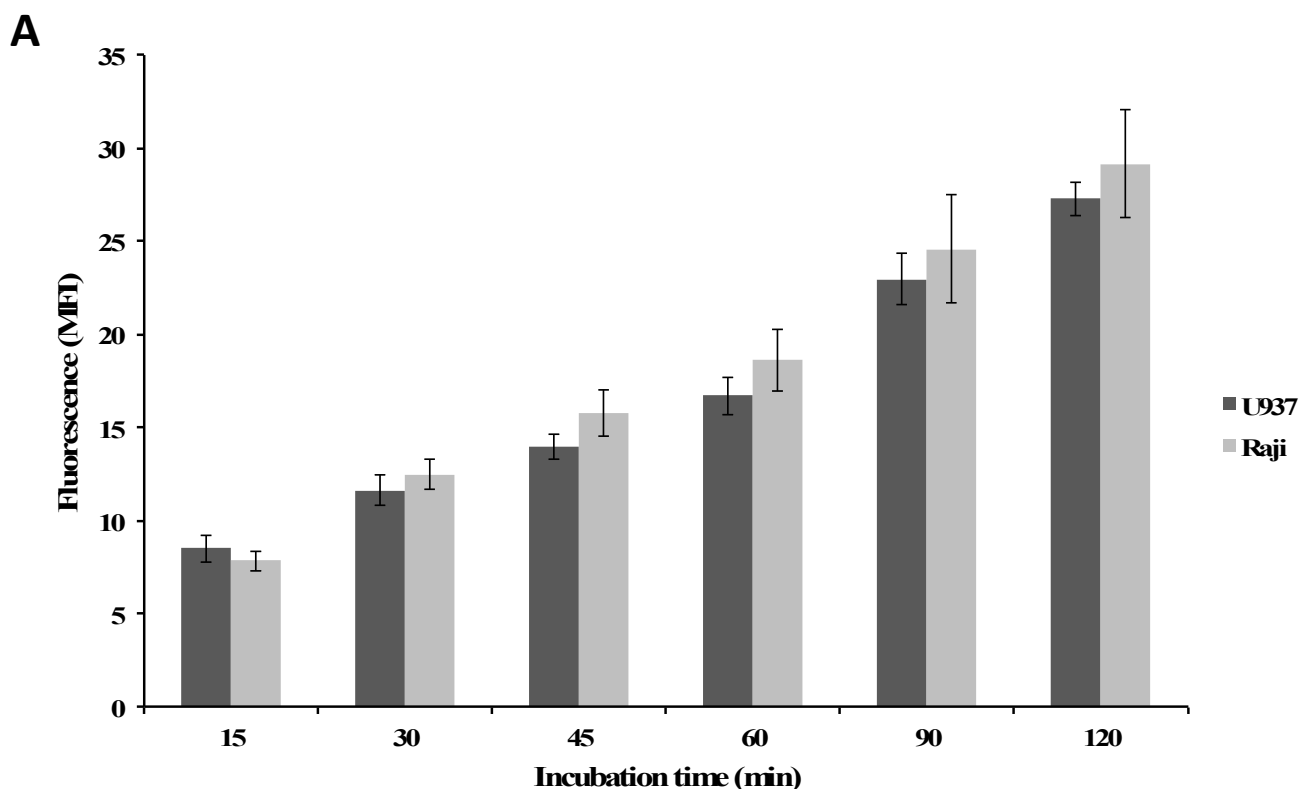
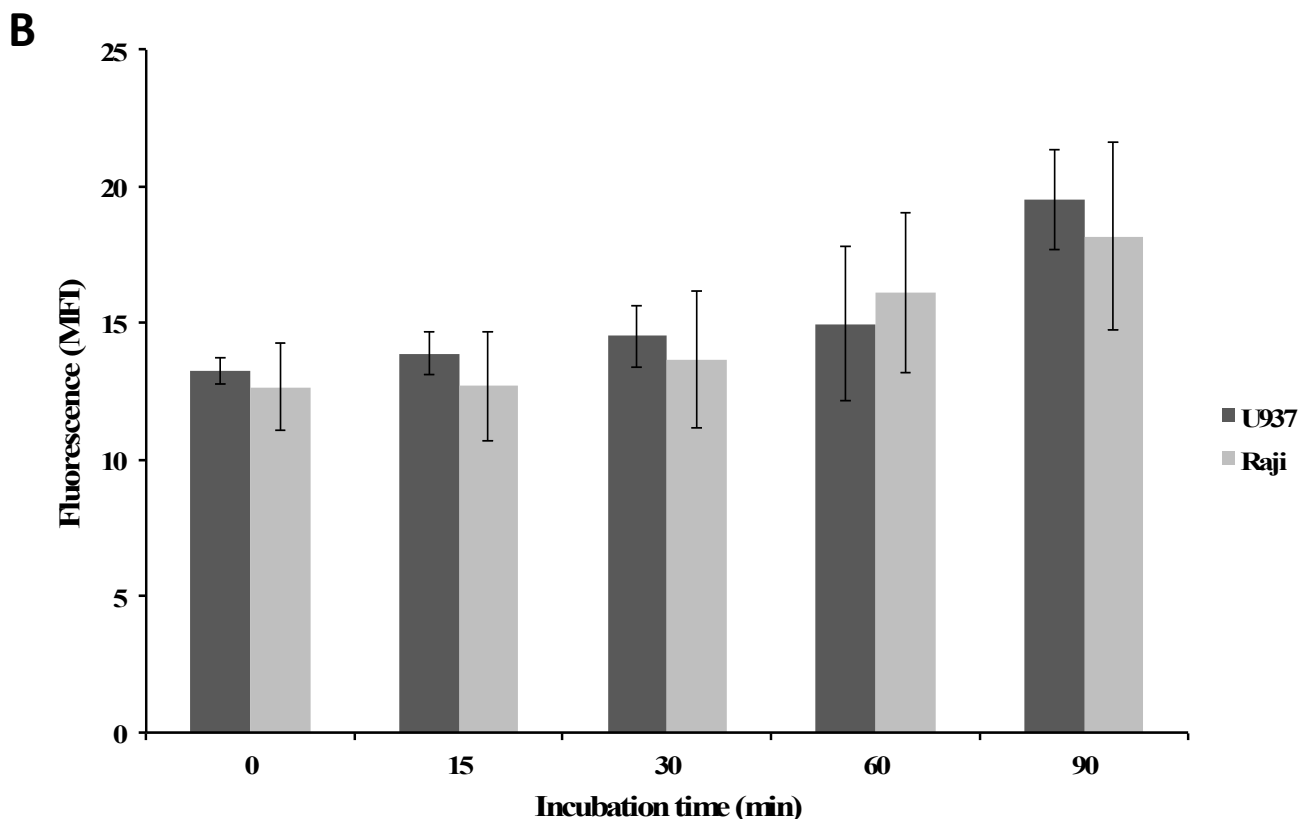


Figure 4. Cont.



2.5. Thiol-Containing Antioxidants Prevent Plumbagin-Induced Apoptosis

As ROS are known to play a key role in apoptosis induction [51], we investigated the effect of antioxidants on ROS generation and apoptotic cell death induction. Using BSO, a GSH depletor, and H_2O_2 as positive controls for ROS generation, our analysis showed that the pre-treatment with DTT [52], NAC [12,15] and Trolox [53] buffers plumbagin-dependent ROS production whereas the metal chelator Tiron [53,54], a hydroxyl radical and superoxide scavenger, remained ineffective as antioxidant agent in both models (Figure 5A,C). Then, we estimated the percentage of apoptosis by analyzing the loss of mitochondrial membrane potential (see “Experimental” section), a marker of the mitochondrial apoptotic pathway [12,50]. Only pre-treatment with DTT or NAC, two thiol-containing antioxidants, prevented cell death, while non-thiol antioxidants, Tiron and Trolox, did not affect apoptosis, although Trolox was able to buffer ROS formation (Figure 5B,D). Cancer cells typically develop alterations of their oxidative status, by showing altered expression patterns of enzymes whose function might depend on thiol modulation [40,42,43,55–57]. Our findings indicate an ability of plumbagin to eventually lead to the modulation of important intracellular functions especially those dominated by thiol modulation, which include also enzymes controlling and/or modulating the cellular redox status in cancer cells.

Figure 5. (A) ROS measurement in U937 after 15 min of treatment with plumbagin using H₂DCFDA. Cells were pre-treated with BSO and different antioxidants (DTT, NAC, Tiron and Trolox) prior to ROS analysis by flow cytometry; (B) Mitochondrial membrane potential was determined in U937 cells 24 h after plumbagin treatment; (C) ROS measurement in Raji cells was performed under the same conditions as used for U937 cells (see point (A)); (D) Mitochondrial membrane potential was determined in Raji cells 24 h after plumbagin treatment. Results are the mean ± SD of at least three independent experiments. For the statistical analysis, results were considered as statistically significant for *p* values * *p* < 0.05, ** *p* < 0.01 and *** *p* < 0.001 when compared to their respective control (black bars for the ROS measurement analysis), and were considered as statistically significant for *p* values §§ *p* < 0.01 and §§§ *p* < 0.001 when compared to cells treated only with the vehicle DMSO.

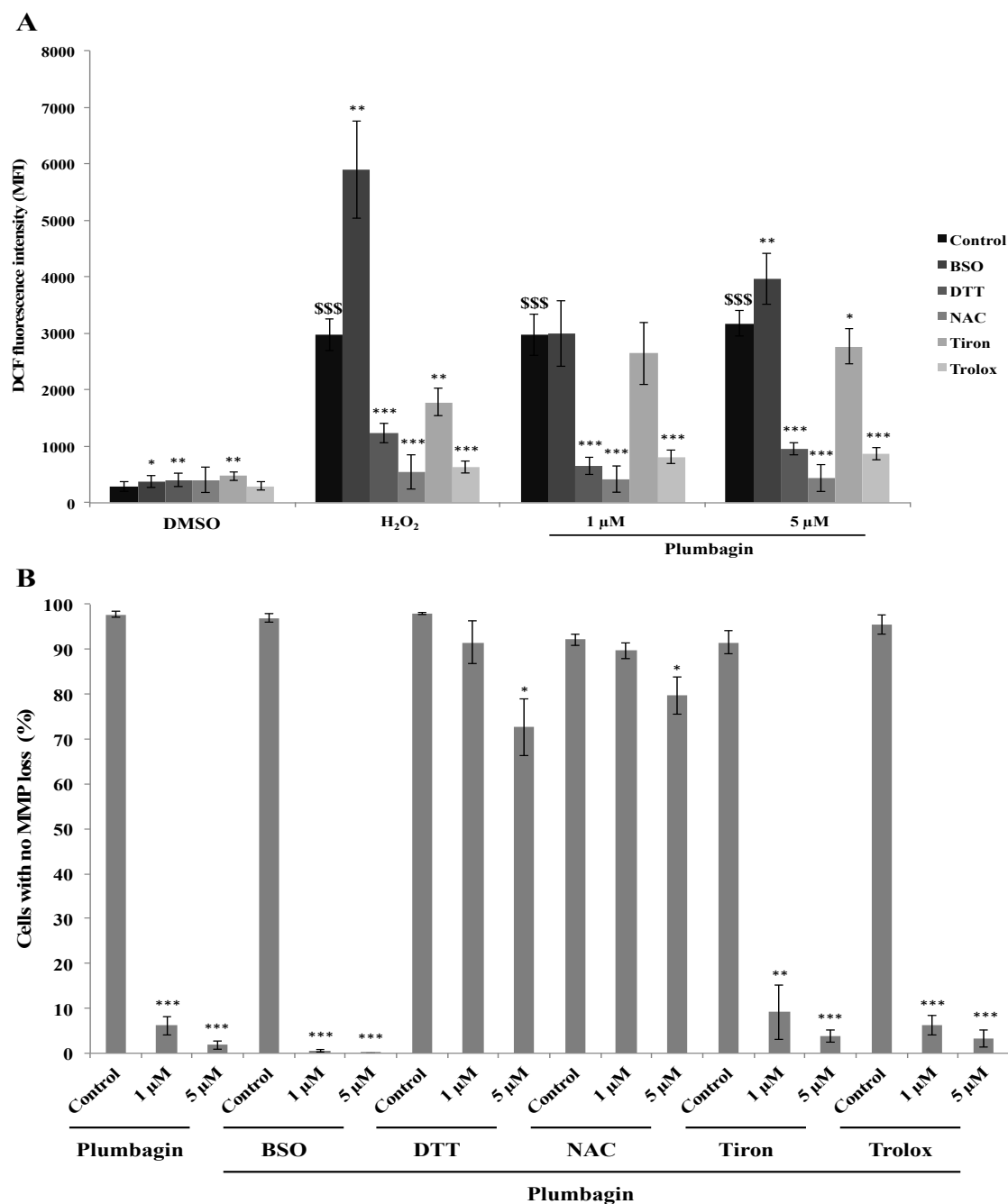
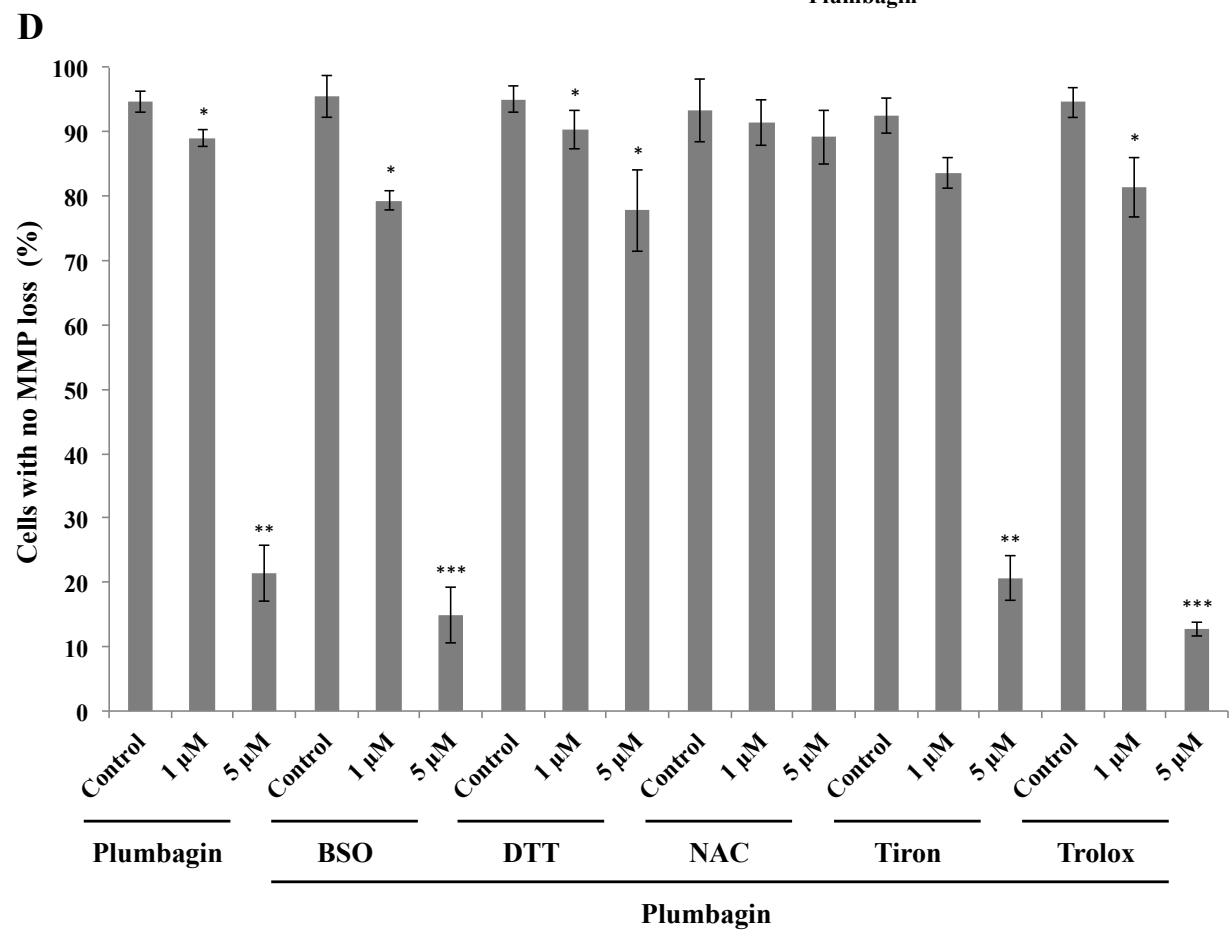
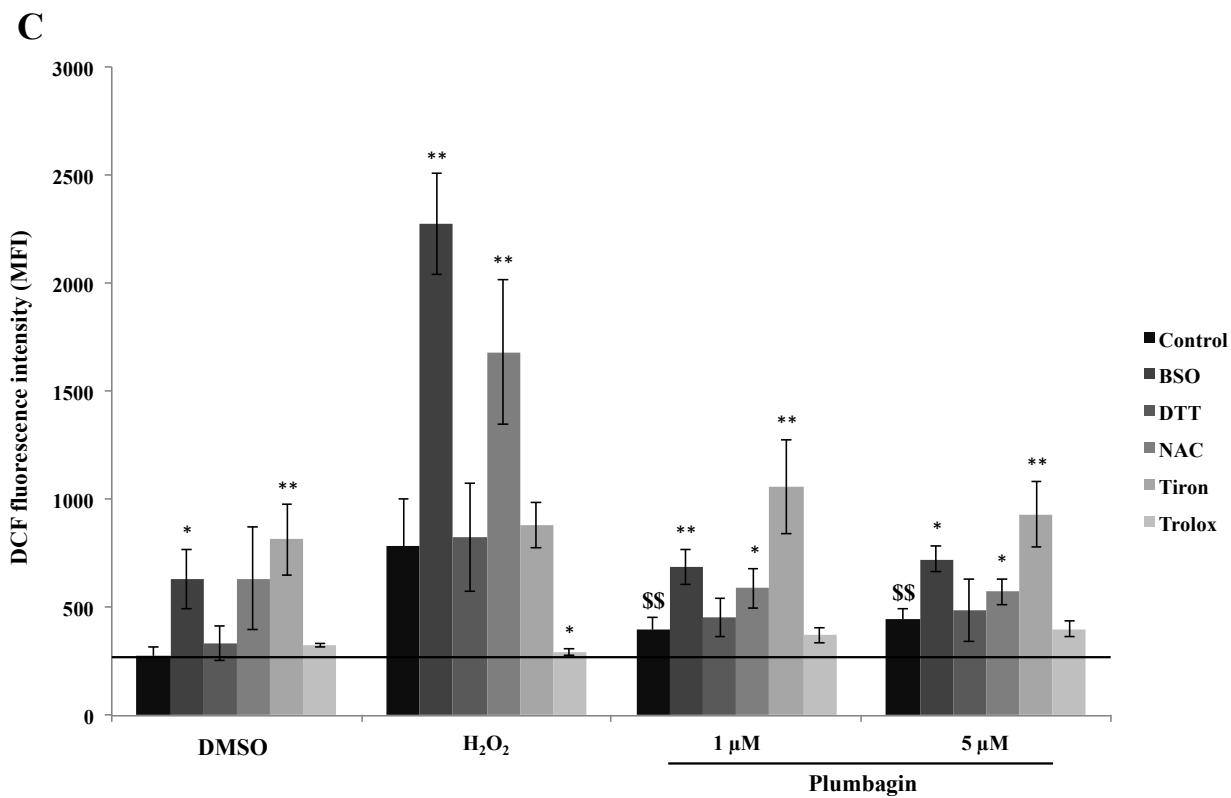


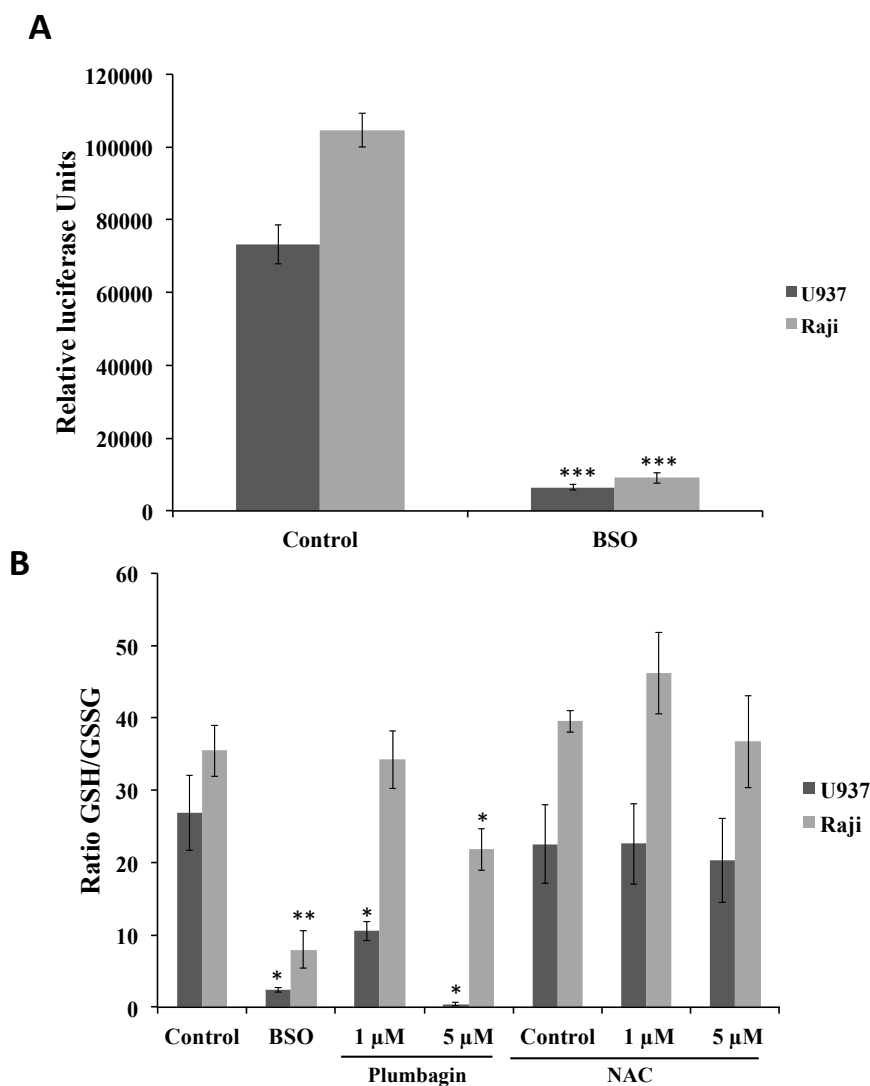
Figure 5. Cont.



2.6. Plumbagin Decreases the Intracellular GSH Level

Next, we investigated the impact of plumbagin on GSH as it has been shown that GSH depletion is a common feature in apoptotic cell death [58]. To elucidate the mechanisms explaining the differential sensitivity, we measured the level of total GSH, which is 30% higher in Raji compared to sensitive U937 cells (Figure 6A). These differential GSH levels could explain the plumbagin-induced ROS production observed in the two selected models (Figures 3 and 5). Then, we analyzed the GSH/GSSG ratio after stimulation with plumbagin using BSO- and NAC-treated cells as controls. Plumbagin decreases the GSH/GSSG ratio in both cell lines in a dose-dependent manner. NAC treatment per se did not significantly alter the GSH/GSSG ratio observed in control cells.

Figure 6. (A) Total glutathione levels (GSH + GSSG) were determined in U937 and Raji cells using a GSH/GSSG-Glo Assay (Promega). Cells pre-treated during 24 h with BSO (1 mM) were used as control; (B) GSH/GSSG ratios of U937 and Raji cells were measured after 1 h of treatment with plumbagin. Cells pre-treated during 24 h with BSO (1 mM) or NAC (10 mM) were used as control. Results are the mean \pm SD of at least three independent experiments. * $p < 0.05$, ** $p < 0.01$ and *** $p < 0.001$ compared to non-treated cells, respectively.



In Raji cells, a 40% decrease is observed at 5 μM compared to a decrease of 60% in U937 cells (Figure 6B). The analysis of reduced GSH by *O*-phthalaldehyde (OPA) assay revealed that a dose of 5 μM of plumbagin is requested to decrease the GSH content by 25% in Raji cells whereas 1 μM is sufficient to reach the same level in U937 cells. 24 h pre-treatment with NAC completely abrogates the previously described depletion of GSH by plumbagin (Table 2).

Table 2. Intracellular GSH level was determined using OPA probe after 1 h of treatment with plumbagin. Cells pre-treated during 24 h with NAC (10 mM) were used as control. Results are the mean \pm SD of at least three independent experiments (values are indicated as a ratio of fluorescence values between treated and control cells). * $p < 0.05$, and ** $p < 0.01$ compared to non-treated cells, respectively.

Treatment	Cell Lines	Control	H ₂ O ₂ (50 μM)	Plumbagin (1 μM)	Plumbagin (5 μM)
Control (DMSO)	U937	100.00	88.38 \pm 17.87	67.34 \pm 9.21 (*)	66.20 \pm 13.26 (*)
	Raji	100.00	94.10 \pm 13.88	88.49 \pm 16.93	80.38 \pm 5.59 (*)
NAC (10 mM)	U937	100.00	89.99 \pm 6.42	92.59 \pm 17.54	85.71 \pm 3.86 (**)
	Raji	100.00	111.36 \pm 11.02	110.76 \pm 8.74	90.85 \pm 14.80

3. Experimental

3.1. Reagents

Plumbagin (Sigma-Aldrich, Bornem, Belgium) was dissolved in dimethyl sulfoxide (DMSO) (Sigma-Aldrich) at a concentration of 100 mM. Subsequent dilutions were made in cell culture medium. Buthionine sulfoximine (BSO), N-acetyl-L-cysteine (NAC), H₂O₂, propidium iodide (PI) and Trolox were purchased from Sigma. Z-VAD-FMK (Calbiochem, San Diego, CA, USA). Tiron was purchased from Alfa Aesar (Karlsruhe, Germany) and dithiothreitol (DTT) from Roche (Prophac, Luxembourg). Dichlorofluorescein diacetate (H₂DCFDA), and *O*-phthalaldehyde (OPA) probes were purchased by Life technologies Invitrogen (ThermoFisher, Alost, Belgium).

3.2. Cell Culture

HL-60 (human promyelocytic leukemia), Jurkat (T-cell leukemia), K562 (human chronic myelogenous leukemia), Raji (Burkitt lymphoma) and U937 (histiocytic lymphoma) cells were cultured in RPMI 1640 medium (Lonza, Verviers, Belgium) supplemented with 10% (*v/v*) fetal calf serum (FCS) (Lonza) and 1% (*v/v*) antibiotic-antimycotic (BioWhittaker, Verviers, Belgium) at 37 °C and 5% of CO₂, humidified atmosphere. Exponentially growing cells were used for plumbagin treatment. Cells treated with DMSO (1 %) were used as control. For specific experiments, Raji and U937 cells were pre-treated with NAC (10 mM) or BSO (1 mM) for 24 h, DTT (100 μM) for 2 h, or with Tiron (10 mM) or Trolox (1 mM) for 1h before plumbagin treatment. Control cells were not pre-treated. Z-VAD-FMK (50 μM , 1 h)

Healthy blood samples were kindly donated as buffy coats by the Red Cross (Luxembourg, Grand Duchy of Luxembourg). By applying diluted (1/3) blood onto a Ficoll layer (GE Healthcare, Diegem, Belgium) followed by centrifugation (500 g, 30 min), mononuclear cells were isolated and collected.

The isolated peripheral blood mononuclear cells (PBMCs) were cultured at 37 °C and 5% CO₂ for 24 h before use.

3.3. Cell Viability Assay

Cancer cells (2×10^5 cells/mL) and PBMCs (2×10^6 cells/mL) were incubated with different concentrations of plumbagin during 24, 48 or 72 h. Cell viability was assessed by trypan blue exclusion test.

3.4. Fluorescence Microscopy

After plumbagin treatment, cells were stained with Hoechst 33342 (Calbiochem) and propidium iodide (Sigma–Aldrich) during 20 min at 37 °C. Labeled cells were analyzed with an inverted Cell M Olympus Microscope (Olympus, Aartselaar, Belgium) and Cell M software.

3.5. Apoptosis Assays

Apoptosis was assessed and estimated by three different assays: (1) analysis of nuclear fragmentation (Hoechst staining and fluorescence microscope observation, performed as previously described [59]); (2) evaluation of phosphatidylserine exposure and (3) evaluation of mitochondrial membrane potential. Evaluation of phosphatidylserine exposure was performed with the Annexin V: FITC Apoptosis Detection Kit I (BD Pharmingen, Erembodegem, Belgium) according to the manufacturer's instructions. Briefly, after 24 h of treatment with different concentrations of plumbagin, 1×10^6 cells were washed with cold phosphate buffered saline (PBS), resuspended in binding buffer and stained with Annexin V-FITC and propidium iodide for 15 min. To evaluate the reduction of mitochondrial membrane potential, plumbagin-treated cells were stained with 50 nM MitoTracker Red CMXRos (Invitrogen) during 20 min at 37 °C according to the manufacturer's protocol. For both approaches, stained samples were analyzed by flow cytometry (FACSCalibur, BD Biosciences, San Jose, CA, USA). Data were recorded using CellQuest and further analyzed by FlowJo software version 8.8.7 (Tree Star Inc, Ashland, OR, USA) available online: <http://www.flowjo.com>.

3.6. Western-Blot

Total proteins extracts were subjected to sodium dodecyl sulfate polyacrylamide gel electrophoresis (SDS–PAGE, 12%) and transferred onto nitrocellulose membranes (Hybond™-P membrane, GE Healthcare). Membranes were pre-hybridized with 5% non-fat milk in PBS 1X containing 0.1% (v/v) Tween 20 (PBS-T) overnight at 4 °C or 1 h at room temperature. Membranes hybridizations with primary antibodies directed against caspase-3, caspase-7, caspase-8, caspase-9 (Cell Signaling, Bioké, Leiden, The Netherlands), Bcl-2 (Calbiochem) and β -actin (Sigma) used as loading control, were carried out in PBS-T containing 5% milk or 5% bovine serum albumin (BSA) for 1 h at room temperature or overnight at 4 °C, according to the providers' protocols. Etoposide-treated U937 cells (VP16, 100 μ M, 4 h) were used as apoptosis positive control and equal loading of samples was controlled using β -actin. After incubation with primary antibodies, membranes were washed and probed with the corresponding secondary (horseradish peroxidase conjugated) antibodies following manufacturers'

instructions for 1 h at room temperature. Proteins of interest were visualized with ECL Plus Western Blotting Detection Reagents (GE Healthcare) using the ImageQuant LAS 4000 Mini (GE Healthcare).

3.7. Evaluation of ROS Production

Raji and U937 cells were treated with plumbagin during 15, 30, 45, 60 or 120 min. 20 min before the end of the treatment, cells were stained at 37 °C with 10 µM of 2',7'-dichlorodihydrofluorescein diacetate (H₂DCFDA) (LifeTechnologies, Gent, Belgium) and analyzed by flow cytometry (FACSCalibur). In the presence of ROS, the non fluorescent cell permeant DCFDA is converted in highly fluorescent 2',7'-dichlorofluorescein (DCF). 50 µM of H₂O₂ for 15 or 30 min were used as an inducer of ROS production (positive control). Relative intracellular ROS levels were depicted as mean fluorescence intensity (MFI).

3.8. Plumbagin Intracellular Uptake and Efflux

Exponentially growing Raji and U937 cells were exposed to 5 µM plumbagin. Plumbagin uptake was assessed by measuring plumbagin intracellular fluorescence from compound-loaded cells after different incubation times (15, 30, 45, 60, 90 and 120 min). At the end of these specific incubation times, cells were collected, centrifuged and re-suspended in fresh medium for further analysis. Efflux of plumbagin was evaluated in the following way, as previously described for doxorubicin [50]. After 30 min of incubation with plumbagin (5 µM), plumbagin-containing medium was removed and cells were re-suspended in fresh medium for recovery [50]. Fluorescence was evaluated immediately (T = 0 min) and after 15, 30, 60, and 90 min. Plumbagin fluorescence was evaluated at the indicated times by flow cytometry using a FACSCalibur, tuned at 488 nm, at standard pass filters; FL2 (FL2 = 585/42 nm). Data were recorded using the CellQuest software and further analyzed with FlowJo.

3.9. Analysis of GSH Content

Reduced (GSH) and oxidized (GSSG) glutathione measurements were performed using the GSH/GSSG-Glo™ Assay kit (Promega, Leiden, The Netherlands). Briefly, after treatment with plumbagin, 5×10^5 cells are collected, centrifuged and resuspended in 1 mL of pre-warmed Hank's Buffered Salt Solution (HBSS). Cells treated with BSO served as a positive control of depletion of GSH content [60]. A volume of 25 µL of the cell suspension is transferred into wells of a 96-well plate. An equivalent volume of appropriate lysis buffer is then added. GSH/GSSG-Glo assay is then performed following manufacturer's instructions. The analysis of cellular GSH content was carried out by staining of the cells with o-phthalaldehyde (OPA), a permanent fluorescent probe. OPA is a direct tool that can interact with small thiol groups (e.g., GSH) in order to form adducts with them. Briefly, Raji and U937 cells were treated with 1 or 5 µM of plumbagin for 1 h. At the end of the incubation time, cells were washed with PBS and incubated with 50 µM OPA for 20 min. OPA fluorescence was evaluated by spectrofluorimetry (SpectraMax Gemini EM, Molecular Devices, Sunnyvale, CA, USA).

3.10. Statistical Analysis

Results from at least three independent experiments were analyzed for statistical significant differences using the Student's *t*-test. They are expressed as the mean \pm SD. *p*-values <0.05 (*), <0.01 (**) and <0.001 (***) were considered as statistically significant.

4. Conclusions

Plumbagin is a natural compound that exerts differential cytotoxicity towards leukemia cancer cells resulting from its modulatory activities on the cellular redox state, however the actual cellular targets of plumbagin in the redox control remain still under debate. ROS increase is commonly detected upon plumbagin treatment. Recently, several studies have pointed at the specific ability of plumbagin to modulate the intracellular thiols. These findings would imply the modulation of the intracellular thiolstat as relevant to trigger the anti-cancer effects of plumbagin, rather than the generation of ROS, which therefore would appear as a merely additional side effect, in the fact not essential for its anticancer activity. Our data seem to support this latter model (Table 3), as apoptosis induced by plumbagin in our sensitive (U937) and less sensitive (Raji) hematopoietic cancer cell models can be prevented only by antioxidants containing thiol species.

Table 3. Summary of the results. A horizontal arrow (\rightarrow) indicates that the antioxidant has no effect on the parameter observed compared to the control. A downward arrow (\searrow) indicates a decrease of the parameter observed compared to the control.

Cell Line	U937				Raji			
Plumbagin model	More sensitive (IC ₅₀ 24 h = 1 μ M)				Less sensitive (IC ₅₀ 24 h = 5 μ M)			
Cell death	Apoptosis							
Plumbagin uptake	Similar incorporation (up to 120 min)							
Plumbagin efflux	No efflux, fluorescence remains constant							
ROS production	Elevated				Moderate			
GSH modulation	GSH modulation depending on their respective IC ₅₀							
Antioxidant classification	Thiol group		Non-thiol group		Thiol group		Non-thiol group	
Antioxidant	DTT	NAC	Tiron	Trolox	DTT	NAC	Tiron	Trolox
ROS production	\searrow	\searrow \searrow	\rightarrow	\searrow	\rightarrow	\rightarrow	\rightarrow	\rightarrow
Apoptosis	\searrow	\searrow	\rightarrow	\rightarrow	\searrow	\searrow	\rightarrow	\rightarrow

There is evidence that plumbagin may directly interact with GSH, by likely a nucleophilic addition, which in turn may contribute to GSH depletion [22,45]. The small intracellular thiol GSH is paradigmatic for a huge group of additional and more complex intracellular thiols potentially targetable by plumbagin, which also includes many structural proteins and enzymes. Tubulin is among the proteins/enzymes known to be bound by plumbagin [61]. Remarkably, thiol modulation is particularly relevant also for the multi-step activation of the pro-apoptotic Bcl-2 family members [62–64]. Strong evidence suggests the modulation of specific Bax (Bcl-2-associated X protein) cysteine residues is critical for the acquisition of its suitable conformation, oligomerization and translocation/insertion into the mitochondrial membrane [65]. It would be relevant in the future to investigate any potential ability of plumbagin to directly interact and thereby modulate *i.e.*, Bax activation. Such interactions can

further contribute to protein derivatization [45]. Glutathione-S-transferases, which control detoxification through the consumption of glutathione (GSH), may also be inactivated by plumbagin. This modulation is paralleled by ROS formation [66]. A previous analysis of GSTP1 level expression, in our lab revealed that the less plumbagin-sensitive Raji cells do not expressed GSTP1 proteins in contrast to the most sensitive U937 cell model here investigated [67,68]. These differential alterations may potentially provide additional hints to may identify the reason of such differences in ROS generation. Taken all together, our and other findings indicate the ability of plumbagin to may eventually lead to the modulation of important intracellular functions dominated by thiol modulation.

Acknowledgments

François Gaascht was supported by a fellowship from the European Union (ITN “RedCat” 215009, Interreg IVa project “Corena”). Marie-Hélène Teiten is supported by Télévie grants (Fonds National de la Recherche Scientifique, Belgium). Claudia Cerella is supported by a “Waxweiler grant for cancer prevention research” from the Action Lions “Vaincre le Cancer”. Research at LBMCC is financially supported by the Fondation de Recherche Cancer et Sang, the Recherches Scientifiques Luxembourg association, the Een Haerz fir kriibskrank Kanner association, the Action Lions Vaincre le Cancer association, the European Union (ITN “RedCat” 215009, Interreg IVa project “Corena”) and the Télévie Luxembourg. Mario Dicato is supported by the National Research Foundation (NRF) by the MEST of Korea for Tumor Microenvironment Global Core Research Center (GCRC) grant [grant No. 2012-0001184].

Author Contributions

All authors conceived and designed the experiments and contributed to data analysis and interpretation of the results. Furthermore they wrote and revised the manuscript.

Conflicts of Interest

The authors declare no conflict of interest.

References

1. Florean, C.; Schneckeburger, M.; Grandjenette, C.; Dicato, M.; Diederich, M. Epigenomics of leukemia: From mechanisms to therapeutic applications. *Epigenomics* **2011**, *3*, 581–609.
2. Karius, T.; Schneckeburger, M.; Dicato, M.; Diederich, M. Micrnas in cancer management and their modulation by dietary agents. *Biochem. Pharmacol.* **2012**, *83*, 1591–1601.
3. Schneckeburger, M.; Diederich, M. Epigenetics offer new horizons for colorectal cancer prevention. *Curr. Colorectal Cancer Rep.* **2012**, *8*, 66–81.
4. Gaascht, F.; Teiten, M.H.; Schumacher, M.; Dicato, M.; Diederich, M. Approche végétale dans le traitement des leucémies. *Corresp. Onco-Hématol.* **2010**, *V*, 102–108.
5. Teiten, M.H.; Gaascht, F.; Dicato, M.; Diederich, M. Anticancer bioactivity of compounds from medicinal plants used in european medieval traditions. *Biochem. Pharmacol.* **2013**, *86*, 1239–1247.

6. Sawadogo, W.R.; Schumacher, M.; Teiten, M.H.; Dicato, M.; Diederich, M. Traditional west african pharmacopeia, plants and derived compounds for cancer therapy. *Biochem. Pharmacol.* **2012**, *84*, 1225–1240.
7. Sawadogo, W.R.; Schumacher, M.; Teiten, M.H.; Cerella, C.; Dicato, M.; Diederich, M. A survey of marine natural compounds and their derivatives with anti-cancer activity reported in 2011. *Molecules* **2013**, *18*, 3641–3673.
8. Teiten, M.H.; Gaascht, F.; Eifes, S.; Dicato, M.; Diederich, M. Chemopreventive potential of curcumin in prostate cancer. *Genes Nutr.* **2010**, *5*, 61–74.
9. Teiten, M.H.; Eifes, S.; Reuter, S.; Duvoix, A.; Dicato, M.; Diederich, M. Gene expression profiling related to anti-inflammatory properties of curcumin in K562 leukemia cells. *Ann. NY Acad. Sci.* **2009**, *1171*, 391–398.
10. Teiten, M.H.; Eifes, S.; Dicato, M.; Diederich, M. Curcumin—the paradigm of a multi-target natural compound with applications in cancer prevention and treatment. *Toxins* **2010**, *2*, 128–162.
11. Teiten, M.H.; Dicato, M.; Diederich, M. Curcumin as a regulator of epigenetic events. *Mol. Nutr. Food Res.* **2013**, *57*, 1619–1629.
12. Kelkel, M.; Cerella, C.; Mack, F.; Schneider, T.; Jacob, C.; Schumacher, M.; Dicato, M.; Diederich, M. ROS-independent JNK activation and multisite phosphorylation of Bcl-2 link diallyl tetrasulfide-induced mitotic arrest to apoptosis. *Carcinogenesis* **2012**, *33*, 2162–2171.
13. Czepukojc, B.; Baltés, A.K.; Cerella, C.; Kelkel, M.; Viswanathan, U.M.; Salm, F.; Burkholz, T.; Schneider, C.; Dicato, M.; Montenarh, M.; *et al.* Synthetic polysulfane derivatives induce cell cycle arrest and apoptotic cell death in human hematopoietic cancer cells. *Food Chem. Toxicol.* **2014**, *64*, 249–257.
14. Cerella, C.; Dicato, M.; Jacob, C.; Diederich, M. Chemical properties and mechanisms determining the anti-cancer action of garlic-derived organic sulfur compounds. *Anticancer Agents Med. Chem.* **2011**, *11*, 267–271.
15. Busch, C.; Jacob, C.; Anwar, A.; Burkholz, T.; Aicha Ba, L.; Cerella, C.; Diederich, M.; Brandt, W.; Wessjohann, L.; Montenarh, M. Diallylpolsulfides induce growth arrest and apoptosis. *Int. J. Oncol.* **2010**, *36*, 743–749.
16. Slingerland, M.; Cerella, C.; Guchelaar, H.J.; Diederich, M.; Gelderblom, H. Cardiac glycosides in cancer therapy: From preclinical investigations towards clinical trials. *Invest. New Drugs* **2013**, *31*, 1087–1094.
17. Juncker, T.; Cerella, C.; Teiten, M.H.; Morceau, F.; Schumacher, M.; Ghelfi, J.; Gaascht, F.; Schnekenburger, M.; Henry, E.; Dicato, M.; *et al.* UNBS1450, a steroid cardiac glycoside inducing apoptotic cell death in human leukemia cells. *Biochem. Pharmacol.* **2011**, *81*, 13–23.
18. Cerella, C.; Dicato, M.; Diederich, M. Assembling the puzzle of anti-cancer mechanisms triggered by cardiac glycosides. *Mitochondrion* **2013**, *13*, 225–234.
19. Ebrahim, W.; Aly, A.H.; Wray, V.; Mandi, A.; Teiten, M.H.; Gaascht, F.; Orlikova, B.; Kassack, M.U.; Lin, W.; Diederich, M.; *et al.* Embellicines A and B: Absolute configuration and NF- κ B transcriptional inhibitory activity. *J. Med. Chem.* **2013**, *56*, 2991–2999.

20. Teiten, M.H.; Mack, F.; Debbab, A.; Aly, A.H.; Dicato, M.; Proksch, P.; Diederich, M. Anticancer effect of altersolanol a, a metabolite produced by the endophytic fungus stemphylium globuliferum, mediated by its pro-apoptotic and anti-invasive potential via the inhibition of NF- κ B activity. *Bioorg. Med. Chem.* **2013**, *21*, 3850–3858.
21. Aung, H.H.; Chia, L.S.; Goh, N.K.; Chia, T.F.; Ahmed, A.A.; Pare, P.W.; Mabry, T.J. Phenolic constituents from the leaves of the carnivorous plant nepenthes gracilis. *Fitoterapia* **2002**, *73*, 445–447.
22. Inbaraj, J.J.; Chignell, C.F. Cytotoxic action of juglone and plumbagin: A mechanistic study using hacat keratinocytes. *Chem. Res. Toxicol.* **2004**, *17*, 55–62.
23. Ahmad, A.; Banerjee, S.; Wang, Z.; Kong, D.; Sarkar, F.H. Plumbagin-induced apoptosis of human breast cancer cells is mediated by inactivation of NF- κ B and Bcl-2. *J. Cell Biochem.* **2008**, *105*, 1461–1471.
24. Hsu, Y.L.; Cho, C.Y.; Kuo, P.L.; Huang, Y.T.; Lin, C.C. Plumbagin (5-hydroxy-2-methyl-1,4-naphthoquinone) induces apoptosis and cell cycle arrest in A549 cells through p53 accumulation via c-Jun NH₂-terminal kinase-mediated phosphorylation at serine 15 *in vitro* and *in vivo*. *J. Pharmacol. Exp. Ther.* **2006**, *318*, 484–494.
25. Manu, K.A.; Shanmugam, M.K.; Rajendran, P.; Li, F.; Ramachandran, L.; Hay, H.S.; Kannaiyan, R.; Swamy, S.N.; Vali, S.; Kapoor, S.; *et al.* Plumbagin inhibits invasion and migration of breast and gastric cancer cells by downregulating the expression of chemokine receptor CXCR4. *Mol. Cancer* **2011**, *10*, 107.
26. Powolny, A.A.; Singh, S.V. Plumbagin-induced apoptosis in human prostate cancer cells is associated with modulation of cellular redox status and generation of reactive oxygen species. *Pharm. Res.* **2008**, *25*, 2171–2180.
27. Srinivas, P.; Gopinath, G.; Banerji, A.; Dinakar, A.; Srinivas, G. Plumbagin induces reactive oxygen species, which mediate apoptosis in human cervical cancer cells. *Mol. Carcinog.* **2004**, *40*, 201–211.
28. Wang, C.C.; Chiang, Y.M.; Sung, S.C.; Hsu, Y.L.; Chang, J.K.; Kuo, P.L. Plumbagin induces cell cycle arrest and apoptosis through reactive oxygen species/c-Jun N-terminal kinase pathways in human melanoma A375.S2 cells. *Cancer Lett.* **2008**, *259*, 82–98.
29. Gomathinayagam, R.; Sowmyalakshmi, S.; Mardhatillah, F.; Kumar, R.; Akbarsha, M.A.; Damodaran, C. Anticancer mechanism of plumbagin, a natural compound, on non-small cell lung cancer cells. *Anticancer Res.* **2008**, *28*, 785–792.
30. Lee, J.H.; Yeon, J.H.; Kim, H.; Roh, W.; Chae, J.; Park, H.O.; Kim, D.M. The natural anticancer agent plumbagin induces potent cytotoxicity in MCF-7 human breast cancer cells by inhibiting a PI-5 kinase for ros generation. *PLoS One* **2012**, *7*, e45023.
31. Nazeem, S.; Azmi, A.S.; Hanif, S.; Ahmad, A.; Mohammad, R.M.; Hadi, S.M.; Kumar, K.S. Plumbagin induces cell death through a copper-redox cycle mechanism in human cancer cells. *Mutagenesis* **2009**, *24*, 413–418.
32. Sandur, S.K.; Pandey, M.K.; Sung, B.; Aggarwal, B.B. 5-hydroxy-2-methyl-1,4-naphthoquinone, a vitamin K3 analogue, suppresses STAT3 activation pathway through induction of protein tyrosine phosphatase, SHP-1: Potential role in chemosensitization. *Mol. Cancer Res.* **2010**, *8*, 107–118.

33. Subramaniya, B.R.; Srinivasan, G.; Sadullah, S.S.; Davis, N.; Subhadara, L.B.; Halagowder, D.; Sivasitambaram, N.D. Apoptosis inducing effect of plumbagin on colonic cancer cells depends on expression of COX-2. *PLoS One* **2011**, *6*, e18695.
34. Sun, J.; McKallip, R.J. Plumbagin treatment leads to apoptosis in human K562 leukemia cells through increased ROS and elevated TRAIL receptor expression. *Leuk. Res.* **2011**, *35*, 1402–1408.
35. Lai, L.; Liu, J.; Zhai, D.; Lin, Q.; He, L.; Dong, Y.; Zhang, J.; Lu, B.; Chen, Y.; Yi, Z.; *et al.* Plumbagin inhibits tumour angiogenesis and tumour growth through the RAS signalling pathway following activation of the VEGF receptor-2. *Br. J. Pharmacol.* **2012**, *165*, 1084–1096.
36. Sinha, S.; Pal, K.; Elkhanany, A.; Dutta, S.; Cao, Y.; Mondal, G.; Iyer, S.; Somasundaram, V.; Couch, F.J.; Shridhar, V.; *et al.* Plumbagin inhibits tumorigenesis and angiogenesis of ovarian cancer cells *in vivo*. *Int. J. Cancer* **2013**, *132*, 1201–1212.
37. Sandur, S.K.; Ichikawa, H.; Sethi, G.; Ahn, K.S.; Aggarwal, B.B. Plumbagin (5-hydroxy-2-methyl-1,4-naphthoquinone) suppresses NF- κ B activation and NF- κ B-regulated gene products through modulation of p65 and ikappabalpha kinase activation, leading to potentiation of apoptosis induced by cytokine and chemotherapeutic agents. *J. Biol. Chem.* **2006**, *281*, 17023–17033.
38. Xu, T.P.; Shen, H.; Liu, L.X.; Shu, Y.Q. Plumbagin from plumbago zeylanica l induces apoptosis in human non-small cell lung cancer cell lines through NF- κ B inactivation. *Asian Pac. J. Cancer Prev.* **2013**, *14*, 2325–2331.
39. Yang, S.J.; Chang, S.C.; Wen, H.C.; Chen, C.Y.; Liao, J.F.; Chang, C.H. Plumbagin activates ERK1/2 and AKT via superoxide, SRC and PI3-kinase in 3T3-11 cells. *Eur. J. Pharmacol.* **2010**, *638*, 21–28.
40. Dhar, S.K.; Tangpong, J.; Chaiswing, L.; Oberley, T.D.; St Clair, D.K. Manganese superoxide dismutase is a p53-regulated gene that switches cancers between early and advanced stages. *Cancer Res.* **2011**, *71*, 6684–6695.
41. Lincoln, D.T.; Ali Emadi, E.M.; Tonissen, K.F.; Clarke, F.M. The thioredoxin-thioredoxin reductase system: Over-expression in human cancer. *Anticancer Res.* **2003**, *23*, 2425–2433.
42. Perry, R.R.; Mazetta, J.A.; Levin, M.; Barranco, S.C. Glutathione levels and variability in breast tumors and normal tissue. *Cancer* **1993**, *72*, 783–787.
43. Skrzycki, M.; Majewska, M.; Podsiad, M.; Czczot, H. Expression and activity of superoxide dismutase isoenzymes in colorectal cancer. *Acta Biochim. Pol.* **2009**, *56*, 663–670.
44. Zhou, J.; Du, Y. Acquisition of resistance of pancreatic cancer cells to 2-methoxyestradiol is associated with the upregulation of manganese superoxide dismutase. *Mol. Cancer Res.* **2012**, *10*, 768–777.
45. Checker, R.; Sharma, D.; Sandur, S.K.; Subrahmanyam, G.; Krishnan, S.; Poduval, T.B.; Sainis, K.B. Plumbagin inhibits proliferative and inflammatory responses of T cells independent of ROS generation but by modulating intracellular thiols. *J. Cell Biochem.* **2010**, *110*, 1082–1093.
46. Castro, F.A.; Mariani, D.; Panek, A.D.; Eleutherio, E.C.; Pereira, M.D. Cytotoxicity mechanism of two naphthoquinones (menadione and plumbagin) in *saccharomyces cerevisiae*. *PLoS One* **2008**, *3*, e3999.
47. SivaKumar, V.; Prakash, R.; Murali, M.R.; Devaraj, H.; Niranjali Devaraj, S. *In vivo* micronucleus assay and gst activity in assessing genotoxicity of plumbagin in swiss albino mice. *Drug Chem. Toxicol.* **2005**, *28*, 499–507.

48. Srinivasan, L.; Mathew, N.; Muthuswamy, K. *In vitro* antifilarial activity of glutathione S-transferase inhibitors. *Parasitol. Res.* **2009**, *105*, 1179–1182.
49. Seshadri, P.; Rajaram, A.; Rajaram, R. Plumbagin and juglone induce caspase-3-dependent apoptosis involving the mitochondria through ROS generation in human peripheral blood lymphocytes. *Free Radic. Biol. Med.* **2011**, *51*, 2090–2107.
50. Cerella, C.; Sobolewski, C.; Chateauvieux, S.; Henry, E.; Schnekenburger, M.; Ghelfi, J.; Dicato, M.; Diederich, M. Cox-2 inhibitors block chemotherapeutic agent-induced apoptosis prior to commitment in hematopoietic cancer cells. *Biochem. Pharmacol.* **2011**, *82*, 1277–1290.
51. Simon, H.U.; Haj-Yehia, A.; Levi-Schaffer, F. Role of reactive oxygen species (ROS) in apoptosis induction. *Apoptosis* **2000**, *5*, 415–418.
52. Seo, H.R.; Seo, W.D.; Pyun, B.J.; Lee, B.W.; Jin, Y.B.; Park, K.H.; Seo, E.K.; Lee, Y.J.; Lee, Y.S. Radiosensitization by celastrol is mediated by modification of antioxidant thiol molecules. *Chem. Biol. Interact.* **2011**, *193*, 34–42.
53. Monticone, M.; Taherian, R.; Stigliani, S.; Carra, E.; Monteghirfo, S.; Longo, L.; Daga, A.; Dono, M.; Zupo, S.; Giaretti, W.; *et al.* NAC, tiron and trolox impair survival of cell cultures containing glioblastoma tumorigenic initiating cells by inhibition of cell cycle progression. *PLoS One* **2014**, *9*, e90085.
54. Yang, J.; Su, Y.; Richmond, A. Antioxidants tiron and N-acetyl-l-cysteine differentially mediate apoptosis in melanoma cells via a reactive oxygen species-independent NF- κ B pathway. *Free Radic. Biol. Med.* **2007**, *42*, 1369–1380.
55. Arrigo, A.P. Gene expression and the thiol redox state. *Free Radic. Biol. Med.* **1999**, *27*, 936–944.
56. Huang, Z.Z.; Chen, C.; Zeng, Z.; Yang, H.; Oh, J.; Chen, L.; Lu, S.C. Mechanism and significance of increased glutathione level in human hepatocellular carcinoma and liver regeneration. *FASEB J.* **2001**, *15*, 19–21.
57. Warner, B.B.; Stuart, L.; Gebb, S.; Wispe, J.R. Redox regulation of manganese superoxide dismutase. *Am. J. Physiol.* **1996**, *271*, L150–L158.
58. Franco, R.; Cidowski, J.A. Glutathione efflux and cell death. *Antioxid. Redox Signaling* **2012**, *17*, 1694–1713.
59. Schumacher, M.; Cerella, C.; Eifes, S.; Chateauvieux, S.; Morceau, F.; Jaspars, M.; Dicato, M.; Diederich, M. Heteronemin, a spongian sesterterpene, inhibits tnf alpha-induced NF-kappa b activation through proteasome inhibition and induces apoptotic cell death. *Biochem. Pharmacol.* **2010**, *79*, 610–622.
60. D'Alessio, M.; Cerella, C.; Amici, C.; Pesce, C.; Coppola, S.; Fanelli, C.; de Nicola, M.; Cristofanon, S.; Clavarino, G.; Bergamaschi, A.; *et al.* Glutathione depletion up-regulates BCL-2 in BSO-resistant cells. *FASEB J.* **2004**, *18*, 1609–1611.
61. Acharya, B.R.; Bhattacharyya, B.; Chakrabarti, G. The natural naphthoquinone plumbagin exhibits antiproliferative activity and disrupts the microtubule network through tubulin binding. *Biochemistry* **2008**, *47*, 7838–7845.
62. Ghibelli, L.; Diederich, M. Multistep and multitask bax activation. *Mitochondrion* **2010**, *10*, 604–613.

63. Nie, C.; Tian, C.; Zhao, L.; Petit, P.X.; Mehrpour, M.; Chen, Q. Cysteine 62 of bax is critical for its conformational activation and its proapoptotic activity in response to H₂O₂-induced apoptosis. *J. Biol. Chem.* **2008**, *283*, 15359–15369.
64. Honda, T.; Coppola, S.; Ghibelli, L.; Cho, S.H.; Kagawa, S.; Spurgers, K.B.; Brisbay, S.M.; Roth, J.A.; Meyn, R.E.; Fang, B.; *et al.* GSH depletion enhances adenoviral bax-induced apoptosis in lung cancer cells. *Cancer Gene Ther.* **2004**, *11*, 249–255.
65. D'Alessio, M.; de Nicola, M.; Coppola, S.; Gualandi, G.; Pugliese, L.; Cerella, C.; Cristofanon, S.; Civitareale, P.; Ciriolo, M.R.; Bergamaschi, A.; *et al.* Oxidative Bax dimerization promotes its translocation to mitochondria independently of apoptosis. *FASEB J.* **2005**, *19*, 1504–1506.
66. Turella, P.; Cerella, C.; Filomeni, G.; Bullo, A.; de Maria, F.; Ghibelli, L.; Ciriolo, M.R.; Cianfriglia, M.; Mattei, M.; Federici, G.; *et al.* Proapoptotic activity of new glutathione S-transferase inhibitors. *Cancer Res.* **2005**, *65*, 3751–3761.
67. Duvoix, A.; Schnekenburger, M.; Delhalle, S.; Blasius, R.; Borde-Chiche, P.; Morceau, F.; Dicato, M.; Diederich, M. Expression of glutathione S-transferase P1–1 in leukemic cells is regulated by inducible AP-1 binding. *Cancer Lett.* **2004**, *216*, 207–219.
68. Karius, T.; Schnekenburger, M.; Ghelfi, J.; Walter, J.; Dicato, M.; Diederich, M. Reversible epigenetic fingerprint-mediated glutathione-s-transferase P1 gene silencing in human leukemia cell lines. *Biochem. Pharmacol.* **2011**, *81*, 1329–1342.

Sample Availability: Plumbagin is a commercially available compound as reported in the “Experimental” section.

© 2014 by the authors; licensee MDPI, Basel, Switzerland. This article is an open access article distributed under the terms and conditions of the Creative Commons Attribution license (<http://creativecommons.org/licenses/by/3.0/>).